AIP | Applied Physics Letters

Absolute second order nonlinear susceptibility of Pt nanowire arrays on MgO faceted substrates with various cross-sectional shapes

Yoichi Ogata and Goro Mizutani

Citation: Appl. Phys. Lett. **103**, 093107 (2013); doi: 10.1063/1.4819916
View online: http://dx.doi.org/10.1063/1.4819916
View Table of Contents: http://apl.aip.org/resource/1/APPLAB/v103/i9
Published by the AIP Publishing LLC.

Absolute second order nonlinear susceptibility of Pt nanowire arrays on MgO faceted substrates with various cross-sectional shapes

Yoichi Ogata and Goro Mizutani[a)]
School of Materials Science, Japan Advanced Institute of Science and Technology, 1-1 Asahidai, Nomi, Ishikawa 923-1292, Japan

(Received 3 June 2013; accepted 16 August 2013; published online 28 August 2013)

We have measured optical second harmonic generation (SHG) intensity from three types of Pt nanowires with 7 nm widths of elliptical and boomerang cross-sectional shapes and with 2 nm width elliptical cross-sectional shapes on the MgO faceted templates. From the SHG intensities, we calculated the absolute value of the nonlinear susceptibility $\chi^{(2)}$ integrated in the direction of the wire-layer thickness. The tentatively obtained bulk $\chi^{(2)}{}_{B}$ of the wire layer was very large, approaching the value of the well-known nonlinear optical material $BaTiO_3$. © *2013 AIP Publishing LLC*. [http://dx.doi.org/10.1063/1.4819916]

Recently, advances of nanofabrication techniques are ready for controlling sizes, shapes, and alignment of nanostructures of a wide range of materials. Experiments have demonstrated the world's smallest wire-width by using leading-edge nanofabrication techniques, and its width was less than 10 nm.[1] One-dimensional metal nanowires show unique optical properties due to the strong anisotropy of their structures. In particular, coherent nonlinear optical phenomenon such as optical second-harmonic generation (SHG) obeys a selection rule depending on the symmetry of the medium's structure.[2–4] Recently, researchers have investigated nonlinear optical properties of nanowires by SHG spectroscopy.[2,3] Understanding of their nonlinear optical properties will provide potential applications to frequency converters.[5]

So far, SHG properties of Au, Cu, and Pt nanowires prepared by shadow deposition method have been reported.[6–8] In earlier studies, Hayashi *et al.* measured SHG intensity from Pt nanowires with 20 nm and 9 nm average widths.[8] We have recently fabricated an array of ~7 nm-width Pt nanowires with elliptical and boomerang cross-sectional shapes and discussed their SHG response.[9] The symmetry of the nanowires' structure influenced sensitively the SHG signal patterns as a function of the sample rotation angle around its surface normal. We have also fabricated an array of Pt nanowires with width of around 2 nm and compared their SHG intensity with those from other nanowires.[10] According to Ref. 10 and our later measurement, the maximum SHG intensity I_{SHG} ($\varphi = 0°$) from the 2 nm width Pt nanowires was 23 times larger than I_{SHG} ($\varphi = 90°$) from the 7 nm width in the *p*-in/*p*-out polarization configuration. Here, the 7 nm-width nanowires had elliptical cross sections. If a large value of nonlinear susceptibility $\chi^{(2)}$ is attained, the development of optical nonlinear materials by multi-layer stacking of the nanowires can be envisioned. Thus, in this study, we will measure the absolute value of the second order nonlinear susceptibility $\chi^{(2)}$ of the three kinds of Pt nanowires by comparing the SHG intensity between the nanowires and a quartz plate.

The details of the preparation of the three kinds of Pt nanowires on a faceted MgO template have been already reported.[9,10] In the following, we report the physical properties of the 2 nm width Pt nanowires obtained afterwards. The width of more than 1000 individual nanowires was measured using the NIH ImageJ analysis software program (Wayne Rasband, National Institutes of Health, USA, http://rsb.info.nih.gov/ij), and the average width of the Pt nanowires was 2.1 nm with a standard deviation of 0.59 nm in a plan-view transmission electron microscope (TEM) image. The resolution of the TEM equipment (HITACHI, H-9000NAR) was 0.18 nm. According to the TEM diffraction pattern, this platinum has *fcc* structure with centrosymmetry. Also the existence of the relatively large moiré patterns in the plan-view TEM image means that the single crystal domain size is as large as 5 nm, although no preferred crystalline orientation was seen with respect to the lattice of the MgO template. Figure 1 shows the TEM image of the cross-section of the Pt nanowires. The cross-sectional shapes of the Pt nanowires on the MgO(210) faceted template are elliptical. Also the facet pitch is seen to be ~11 nm. In Fig. 1, one of the nanowires has been blown off by the Ar ion beam during the preparation of

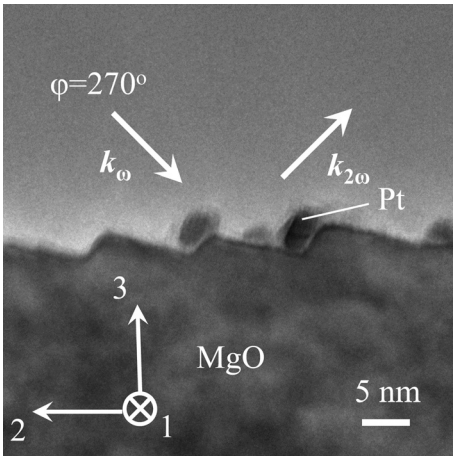

FIG. 1. Cross-sectional TEM image of the Pt nanowires with 2 nm width on the MgO (210) faceted substrate surface with saw-tooth shapes. The cross-sectional shapes of the Pt nanowires seen in dark contrast are like tilted ellipses. As seen in the image, one of the nanowires has been blown off during the preparation of the TEM sample. Two arrows indicate the wave vectors, $\boldsymbol{k}_\omega$ and $\boldsymbol{k}_{2\omega}$, of the fundamental and reflected SHG light beams for $\varphi = 270°$.

a)Author to whom correspondence should be addressed. Electronic mail: mizutani@jaist.ac.jp

the TEM sample. The reason for the blur of the edges of the substrate and the cross section of the nanowires is the thickness of the cross-sectional sample, and it is about 50–100 nm. The images seen from 1:[001] direction may be blurred by the superposition of the images depending on the depth.

The measurement system of the SHG intensity has also been described in our previous work.[10] A frequency-doubled mode-locked Nd^{3+}:YAG laser with light pulses of photon energy 2.33 eV, time duration of 30 ps, and a repetition rate of 10 Hz was used as the excitation source. The average incident pulse energy was set at 120 μJ. The beam spot size on the sample surface was 2 mmφ and thus the fluence was 38 mJ/cm^2. The incidence angle was 45°. A 2ω cut filter was placed in front of the light source to remove residual light at harmonic frequencies generated prior to the interaction with the samples. To measure the azimuthal angle dependence of the SHG intensity, the sample was mounted on a rotation stage. We also compared the maximum SHG intensity $I_{SHG,Pt/MgO}$ of the nanowires with the SHG intensity $I_{SHG,\alpha-SiO2}$ of a z-cut wedged quartz plate (α-SiO_2(0001)) using the same set up in order to determine the absolute value of $\chi^{(2)}$ of the Pt nanowires. Here, the samples were slided and switched on a translational stage. We accumulated the SHG intensity from two hundred thousand Pt nanowires in the direction perpendicular to the nanowire axis inside the spot of the incident light. An ω cut filter was placed after the sample stage to remove the incident light. The detection was made at the photon energy of 4.66 eV with a photomultiplier. The averaged SHG intensity I_{SHG} was obtained by accumulating the signals for 100 000 excitation pulses. The bulk $\chi^{(2)}$ value of α-SiO_2 is well-known in the literature.[11] The excitation power-dependence of the SHG intensity was measured by varying the excitation power from 53 to 160 μJ per pulse. The SHG intensity data fit a quadratic function (not shown). The quadratic power dependence confirms the second-order nature of the measured signal.

We have done a phenomenological analysis of the SHG intensity patterns using a least squares fitting program.[12] We have calculated SHG intensity patterns for each nonlinear susceptibility element using Maxwell's equations. For the calculation, the nanowire arrays are assumed to be a homogeneous dielectric film. The total SHG intensity was a linear combination of these SHG intensity patterns with each term multiplied by the corresponding nonlinear susceptibility element. Finally, the total SHG intensity patterns were fitted to the experimental patterns by varying each nonlinear susceptibility element as fitting parameters. An analysis by more rigorous approach is also possible and has been described by Dadap.[4]

In the previous study, we determined the most effective nonlinear susceptibility element for each type of nanowire. According to the theoretical decomposed calculation patterns, the contribution of $\chi^{(2)}{}_{223}$ strongly dominated in the 7 nm width types. As seen in the decomposition of the SHG intensity patterns from the 2 nm-width nanowire array into contribution of different $\chi^{(2)}$ elements in Figs. 2(a)–2(d), the contribution of $\chi^{(2)}{}_{113}$ is the strongest for this 2 nm-width wires.[10] We also note that the SHG response from the bare MgO(210) faceted surface was at the noise level. Here, the numbers 1, 2, and 3 denote the [001], [1$\bar{1}$0], [110] directions on the MgO (110) faceted substrates and the [001], [1$\bar{2}$0], [210] directions on the MgO(210) facetted substrate, respectively.

We first define the relation between the reflected SHG light intensity and the nonlinear susceptibility $\chi^{(2)}$ of the nanowire layers. Here, we assume that our wire layers can be regarded as a uniform nonlinear dielectric layer, considering that their structural sizes are much smaller than the wavelength of light. Bloembergen and Pershan gave a relation between the reflected SHG light intensity and the nonlinear susceptibility $\chi^{(2)}$ for three-layered dielectric model with the middle nonlinear layer of thickness d.[13] The p-polarized SHG electric field E_{SHG} generated by the $\chi^{(2)}{}_{XXZ}$ element of the nano-structured metals is given as

$$E^R = \frac{i2\omega}{c}\frac{\chi^{(2)}_{XXZ}d}{\tilde{\varepsilon}_S}F_X(2\omega)F_X(\omega)F_Z(\omega)E_{0X}E_{0Z}, \qquad (1)$$

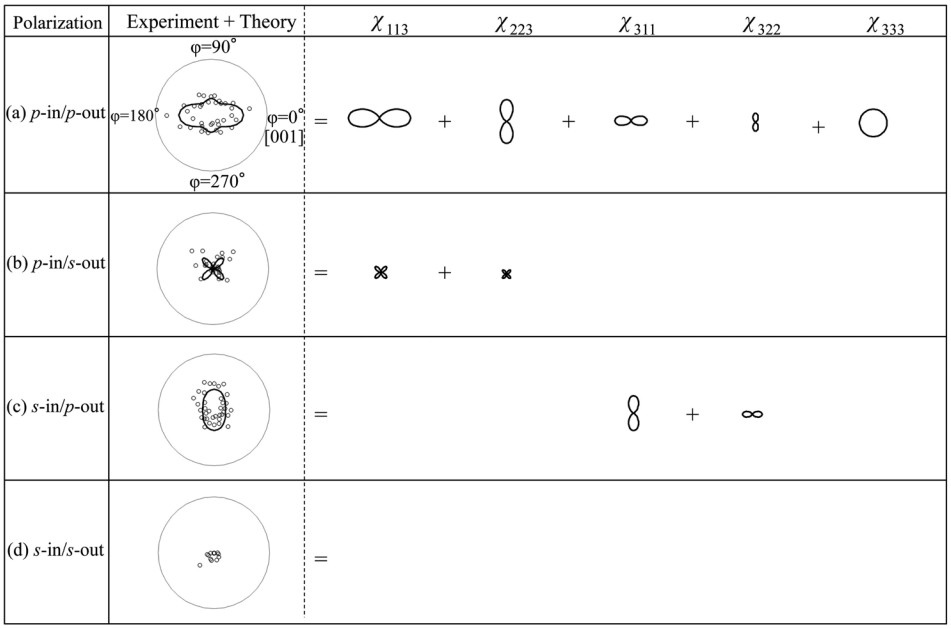

FIG. 2. Calculated SHG intensity patterns decomposed into the contribution of each nonlinear susceptibility element from 2 nm width Pt nanowire arrays. Intensities are in arbitrary but common units in the same row.

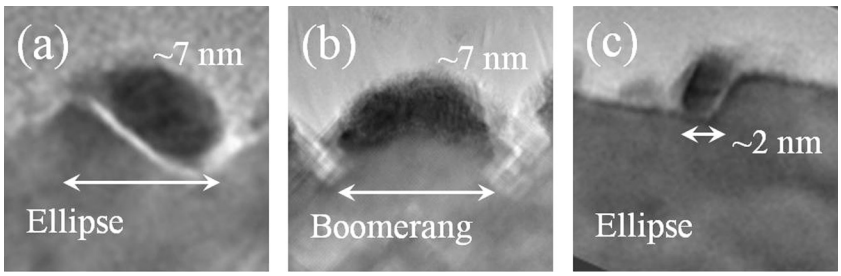

FIG. 3. Cross sectioned TEM images of the Pt nanowires with (a) elliptic, (b) boomerang-like cross-sectional shapes and with (c) ~2 nm width, respectively.

$$F_X(2\omega) = \frac{1}{\sqrt{\tilde{\varepsilon}_R^{2\omega}}\cos\theta_T^{2\omega} + \sqrt{\tilde{\varepsilon}_T^{2\omega}}\cos\theta_R^{2\omega}} \times \left(\sqrt{\frac{\tilde{\varepsilon}_T^{2\omega}}{\tilde{\varepsilon}_S^{\omega}}}\frac{\tilde{\varepsilon}_R^{2\omega}}{\tilde{\varepsilon}_M^{2\omega}}\sin^2\theta_R^{2\omega} - \cos\theta_T^{2\omega}\cos\theta_S^{\omega}\right), \quad (2)$$

$$F_X(\omega) = \frac{\cos\theta_T^{\omega} + \sqrt{\frac{\tilde{\varepsilon}_T^{\omega}}{\tilde{\varepsilon}_S^{\omega}}}\cos\theta_S^{\omega}}{\cos\theta_T^{\omega} + \sqrt{\frac{\tilde{\varepsilon}_T^{\omega}}{\tilde{\varepsilon}_R^{\omega}}}\cos\theta_R^{\omega}}, \quad (3)$$

$$F_Z(\omega) = \frac{\cos\theta_R^{\omega}\left(\cos\theta_S^{\omega} + \sqrt{\frac{\tilde{\varepsilon}_S^{\omega}}{\tilde{\varepsilon}_T^{\omega}}}\cos\theta_T^{\omega}\right)}{\cos\theta_S^{\omega}\left(\cos\theta_R^{\omega} + \sqrt{\frac{\tilde{\varepsilon}_R^{\omega}}{\tilde{\varepsilon}_T^{\omega}}}\cos\theta_T^{\omega}\right)}. \quad (4)$$

Here, suffices X and Z indicate the laboratory coordinate. The plane of incidence is in the X-Z plane and Z is normal to the substrate face. $\tilde{\varepsilon}_R^{\omega}$, $\tilde{\varepsilon}_T^{\omega}$, and $\tilde{\varepsilon}_S^{\omega}$ are the relative permittivities of the top, bottom media, and the middle medium (wire-layer) at frequencies ω, while $\tilde{\varepsilon}_R^{2\omega}$, $\tilde{\varepsilon}_T^{2\omega}$, and $\tilde{\varepsilon}_M^{2\omega}$ are those at frequencies 2ω. θ_R^{ω}, θ_T^{ω}, and θ_S^{ω} are the angles between the surface normal direction and the wave vectors of reflected, transmitted, and homogeneous waves at frequency ω, and $\theta_R^{2\omega}$ and $\theta_T^{2\omega}$ are those of reflected and trasmitted at frequency 2ω. $F(2\omega)$ and $F(\omega)$ are Fresnel factors at the second-harmonic and the fundamental frequencies, respectively. These factors depend weakly on the relative permittivity $\tilde{\varepsilon}_S^{\omega}$ and $\tilde{\varepsilon}_M^{2\omega}$ of the media. The top layer is the air in our study so that we have $\tilde{\varepsilon}_R^{\omega} \approx \tilde{\varepsilon}_R^{2\omega}$ and $\theta_R^{\omega} \approx \theta_R^{2\omega}$.

The averaged SHG intensity from the 2 nm width Pt nanowires in the *p*-in/*p*-out polarization configuration at $\varphi = 0°$ was 4.3 times as high as that from the α-SiO_2(0001) sample in the reflection geometry. This fact is worth attention because SHG is considered to come from the thickness of several hundreds of nanometers in the α-SiO_2(0001) sample, while it comes from ~4 nm thickness of the Pt nanowires. According to Fig. 2, the maximum SHG intensity from the 2 nm width Pt nanowires occurs at the azimuthal angle of $\varphi = 0°$ in the *p*-in/*p*-out polarization configuration. The contribution of $\chi^{(2)}{}_{113}$ strongly dominates the SHG response of the 2 nm nanowires.[14] Thus, we calculated the absolute value of $\chi^{(2)}{}_{113}$ using a least squares fitting program.[15] By measuring the ratio of the SHG signal from the sample to that from the crystalline quartz, the absolute value of $\chi^{(2)}$ of the nanowire sample was determined. Generally, Guyot-Sionnest *et al.* have defined the surface nonlinear susceptibility $\chi^{(2)}{}_S$ by integrating the depth dependent susceptibility in the directions normal to the surface.[16] For our three-layered dielectric model, the $\chi^{(2)}{}_{S,\,113}$ can be written as

$$\chi^{(2)}_{S,113} = \frac{\chi^{(2)}_{B,113B,113} \cdot d}{\tilde{\varepsilon}_S^{\omega}}. \quad (5)$$

If we rewrite Eq. (1) using this relation, $\tilde{\varepsilon}_S^{\omega}$ and d disappears explicitly in Eq. (1). Hence, the value of the nonlinear susceptibility $\chi^{(2)}{}_S$ can be directly obtained from the experiment. The obtained $\chi^{(2)}{}_S$ values for the surface of Pt nanowires are given in Table I.

Generally, we cannot define macroscopic bulk $\chi^{(2)}{}_B$ appearing in Eq. (5) for a composite film like the ones in this study. In this work, we calculate and discuss tentative $\chi^{(2)}{}_B$ values. The thickness d is assumed to be 4 nm from the cross-sectional TEM image in Fig. 1. The tentative linear $\tilde{\varepsilon}_S^{\omega}$ value of the wire-layer was obtained by using the volume average of the three dielectric functions, ε_{ω}(Pt), ε_{ω}(SiO), ε_{ω}(MgO) and ε_0(vacuum), taken from the data by Palik.[17] The volume-averaged dielectric constants $\tilde{\varepsilon}_S^{\omega}$ for the wire-layer were determined to be $-1.4 + 5.9i$, $-3.1 + 7.9i$, and $1.5 + 2.5i$ at $\hbar\omega = 2.33$ eV for the 7 nm-width elliptic, boomerang shaped, and 2 nm-elliptic nanowires, respectively. Then the tentative $\chi^{(2)}{}_B$ values for the bulk for the 2 nm-width nanowire in Fig. 3(c) was $\chi_{B,113} = 16 \times 10^{-12}$[m/V] as shown in Table I.

We calculated tentatively the bulk $\chi^{(2)}{}_B$ value per unit volume appearing in Eq. (5), only to compare them with the

TABLE I. The absolute values of $\chi^{(2)}$ for Pt nanowires with (a) elliptic and (b) boomerang cross-sectional shapes and (c) 2 nm widths. $\tilde{\varepsilon}_S$ is a tentative dielectric constant at the fundamental frequency ω estimated by the volume average of the dielectric constants of the constituent materials in the nanowire layers. $\chi^{(2)}{}_S$ and $\chi^{(2)}{}_B$ are the absolute values of nonlinear susceptibilities for the surface and bulk layers, respectively.

Sample	Tentative $\tilde{\varepsilon}_S$	$\lvert\chi^{(2)}{}_S(\times 10^{-20}[\mathrm{m^2/V}])\rvert$	Tentative $\lvert\chi^{(2)}{}_B(\times 10^{-12}[\mathrm{m/V}])\rvert$
(a) Elliptic, 7 nm	$-1.4 + 5.9$i	0.41	6.2
(b) Boomerang, 7 nm	$-3.1 + 7.9i$	1.3	27
(c) Elliptic, 2 nm	$1.5 + 2.5i$	2.2	16

bulk value of a well-known nonlinear optical crystal. Tentative $\chi^{(2)}{}_{B}$ values for the other two types of Pt nanowires as shown in Figs. 3(a) and 3(b) with elliptical and boomerang-like cross-sectional shapes are also given in Table I, and they are 0.39 and 1.7 times that of 2 nm width wires. The tentative $\chi^{(2)}{}_{B}$ values of the three nanowires are indeed different, but the SHG intensity from the nanowires depends rather on the volume-averaged dielectric constant $\tilde{\varepsilon}_S^{\omega}$. Namely, small $\tilde{\varepsilon}_S^{\omega}$ makes $\chi^{(2)}{}_{S,\,113}$ large and then makes E_{SHG} large.

The conversion efficiency of the fundamental into SHG photons, in the present experiments, was around 10^{-13} at maximum. The efficiency is not small if it comes from a single layer of nanowires. The absolute value of the tentative $\chi^{(2)}{}_{B,113}$ for the bulk is as large as that of the well-known nonlinear optical compound $BaTiO_3$ with $\chi^{(2)}{}_{ZXX} = (-36 \pm 2.8) \times 10^{-12}$ [m/V].[10] The fact suggests that the development of giant permeable nonlinear optical materials consisting of multi-layer stacked 2 nm width Pt nanowires can be expected in the near future.

In summary, we have observed SHG intensities from Pt nanowires with elliptical and boomerang-like cross-sectional shapes, and with widths as small as 2 nm, on a faceted MgO template. We then compared the SHG intensity of the nanowires with that of a quartz plate (α-SiO_2(0001)). The nonlinear optical susceptibility for the surface of these nanowires were $\chi^{(2)}{}_{S,223} = 0.41 \times 10^{-20}$ [m^2/V] in elliptical type with 7 nm thickness, $\chi^{(2)}{}_{S,223} = 1.3 \times 10^{-20}$ [m^2/V] in boomerang type, and $\chi^{(2)}{}_{S,113} = 2.2 \times 10^{-20}$ [m^2/V] in 2 nm width type. The tentative bulk $\chi^{(2)}{}_{B}$ of these nanowire layers were of nearly the same value to that of the famous nonlinear optical compound $BaTiO_3$.

This work was conducted in Kyoto-Advanced Nanotechnology Network, supported by "Nanotechnology Network" of the Ministry of Education, Culture, Sports, Science and Technology (MEXT), Japan. We would like to thank M. Katayama of JAIST Nanotechnology Center for the TEM observation and Dr. Y. Miyauchi of National Defense Academy of Japan for valuable support and advice. This work was supported in part by a Grant-in-Aid for Science Research (c) of Japan Society for the Promotion of Science (#23540363).

[1]S. Danylyuk, L. Juschkin, S. Brose, H. S. Kim, J. Moers, P. Loosen, and D. Gruetzmacher, *in Frontiers in Electronic Materials: A Collection of Extended Abstracts of the Nature Conference Frontiers in Electronic Materials, Aachen, Germany, 17–20 June 2012*, edited by J. Heber, D. Schlom, Y. Tokura, R. Waser, and M. Wuttig (Wiley-VCH Verlag, Weinheim, Germany, 2012), pp. 430–431.
[2]R. Grange, J.-W. Choi, C.-L. Hsieh, Y. Pu, A. Magrez, R. Smajda, L. Forro, and D. Psaltis, Appl. Phys. Lett. **95**, 143105 (2009).
[3]F. Dutto, C. Raillon, K. Schenk, and A. Radenovic, Nano Lett. **11**, 2517 (2011).
[4]J. I. Dadap, Phys. Rev. B **78**, 205322 (2008).
[5]J. C. Johnson, H. Yan, R. D. Schaller, P. B. Petersen, P. Yang, and R. J. Saykally, Nano Lett. **2**, 279 (2002).
[6]T. Kitahara, A. Sugawara, H. Sano, and G. Mizutani, Appl. Surf. Sci. **219**, 271 (2003).
[7]K. Locharoenrat, H. Sano, and G. Mizutani, J. Lumin. **128**, 824 (2008).
[8]N. Hayashi, K. Aratake, R. Okushio, T. Iwai, A. Sugawara, H. Sano, and G. Mizutani, Appl. Surf. Sci. **253**, 8933 (2007).
[9]Y. Ogata and G. Mizutani, Phys. Res. Int. **2012**, 969835.
[10]Y. Ogata, Y. Iwase, Y. Miyauchi, and G. Mizutani, *in 2011 11th IEEE International Conference on Nanotechnology (IEEE-NANO), Oregon, USA, 15–18 August 2011*, edited by IEEE (IEEE, Oregon, USA, 2011), pp. 1661–1664.
[11]Y. R. Shen, *The Principles of Nonlinear Optics* (Wiley, New York, 1984), p. 101.
[12]E. Kobayashi, G. Mizutani, and S. Ushioda, Jpn. J. Appl. Phys., Part 1 **36**, 7250 (1997).
[13]N. Bloembergen and P. S. Pershan, Phys. Rev. **128**, 606, (1962).
[14]Y. Ogata and G. Mizutani, *in Frontiers in Electronic Materials: A Collection of Extended Abstracts of the Nature Conference Frontiers in Electronic Materials, Aachen, Germany, 17–20 June 2012*, edited by J. Heber, D. Schlom, Y. Tokura, R. Waser, and M. Wuttig (Wiley-VCH Verlag, Weinheim, Germany, 2012), pp.438–439.
[15]M. Omote, H. Kitaoka, E. Kobayashi, O. Suzuki, K. Aratake, H. Sano, G. Mizutani, W. Wolf, and R. Podloucky, J. Phys. Condens. Matter **17**, S175 (2005).
[16]P. Guyot-Sionnest, W. Chen, and Y. R. Shen, Phys. Rev. B **33**, 8254 (1986).
[17]E. D. Palik, *Handbook of Optical Constants of Solid* (Academic Press, Boston, 1985).